

Supporting Information

10.1073/pnas.0803727105

SI Methods

Sternberg Item Recognition Paradigm (SIRP). Please see Fig. S2 for a schematic depiction of the SIRP protocol. For each task block, participants were presented with a prompt, “Learn”, and then following a 0.5-s delay, they were shown a memory set comprised of one (1D), three (3D), or five (5D) digits for 6 s. This was followed by a “probe epoch”, which lasted 38 s, and consisted of a series of 14 probe digits presented for 1.1 s with a jittered intertrial interval of ≤ 1.6 s. Participants used a button box to indicate whether each probe digit was a member of the memory set (“target”) or not (“foil”). Within each block, half of the items were targets and the other half were foils. For each participant, target- and foil-button responses were randomly assigned to the right or left thumbs. The stimuli were projected onto a screen positioned on the head coil. Each of 3 runs contained 2 blocks of each of the 3 load conditions (1D, 3D, and 5D), presented in pseudorandom order, with the blocks of each load condition alternating with fixation (baseline) resting periods. Participants were instructed to respond as quickly and accurately as possible and were told that they would receive a bonus of 5 cents for each correct response in addition to a base rate of pay. Each run lasted 6 min.

Functional Image Preprocessing. Functional images were realigned to three-dimensional structural images by using INRIalign, a

motion correction algorithm unbiased by local signal changes (1, 2). Slice-timing correction was performed after realignment to account for possible errors related to the temporal variability in the acquisition of fMRI datasets. Data were spatially normalized (3) into the standard Montreal Neurological Institute (MNI) space and spatially smoothed with a $9 \times 9 \times 9$ mm³ full width at half-maximum Gaussian kernel. Comparison of fMRI data across the 4 sites indicated consistent patterns of load-dependent activation in the DLPFC of patients and control subjects.*

Signal-to-Fluctuation-Noise Ratio Covariate. To further control for scanner differences, a signal-to-fluctuation-noise ratio (SFNR) value was calculated for each subject and also entered as a covariate (4). Briefly, mean-signal intensity was calculated for each gray matter voxel (determined by an automated segmentation algorithm by using the SPM5 MNI templates) across the time points of the fixation epoch at the start of each run. This value was divided by the variance in signal intensity at that voxel, and all voxels were averaged to generate a mean SFNR value. The values for each run were then averaged to generate a SFNR covariate for each participant.

*Gollub RL, et al., *Neuroscience* 2007, Society for Neuroscience Annual Meeting, November 3–7, 2007, San Diego, CA.

1. Freire L, Mangin JF (2001) Motion correction algorithms may create spurious brain activations in the absence of subject motion. *NeuroImage* 14:709–722.
2. Freire L, Roche A, Mangin JF (2002) What is the best similarity measure for motion correction in fMRI time series? *IEEE T Med Imaging* 21:470–484.
3. Ashburner J, Friston KJ (1999) Nonlinear spatial normalization using basis functions. *Hum Brain Mapp* 7:254–266.

4. Friedman L, Glover GH (2006) Reducing interscanner variability of activation in a multicenter fMRI study: Controlling for signal-to-fluctuation-noise-ratio (SFNR) differences. *NeuroImage* 33:471–481.

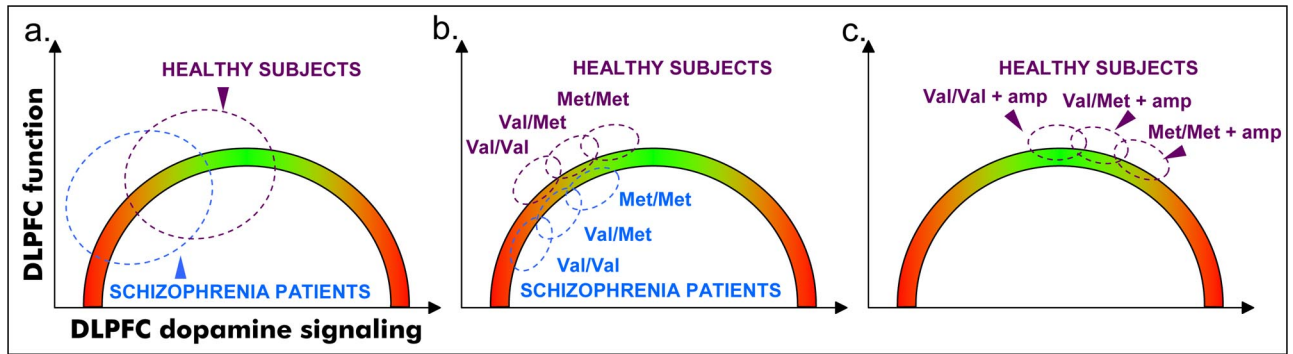


Fig. S1. The canonical inverted U-shaped relationship between dorsolateral prefrontal cortex (DLPFC) function and dopamine signaling. Dopamine signaling that is greater or less than optimal for a particular task results in impaired DLPFC (and hence working memory) function. (a) As a group, schizophrenia patients are believed to have reduced dopamine signaling relative to healthy participants, which may contribute to working memory dysfunction. (b) COMT genotype further stratifies the position of patients and healthy participants on the curve, because of the low activity (decreased dopamine breakdown) of the Met allele and high activity of the Val allele. (c) Administration of amphetamine (amp), a drug that augments dopamine signaling, shifts healthy individuals to the right on the curve, resulting in improved prefrontal function for Val allele carriers but reduced prefrontal function for Met homozygotes [modified from Mattay VS, et al. (2003) *Proc Natl Acad Sci USA* 100:6186–6191].

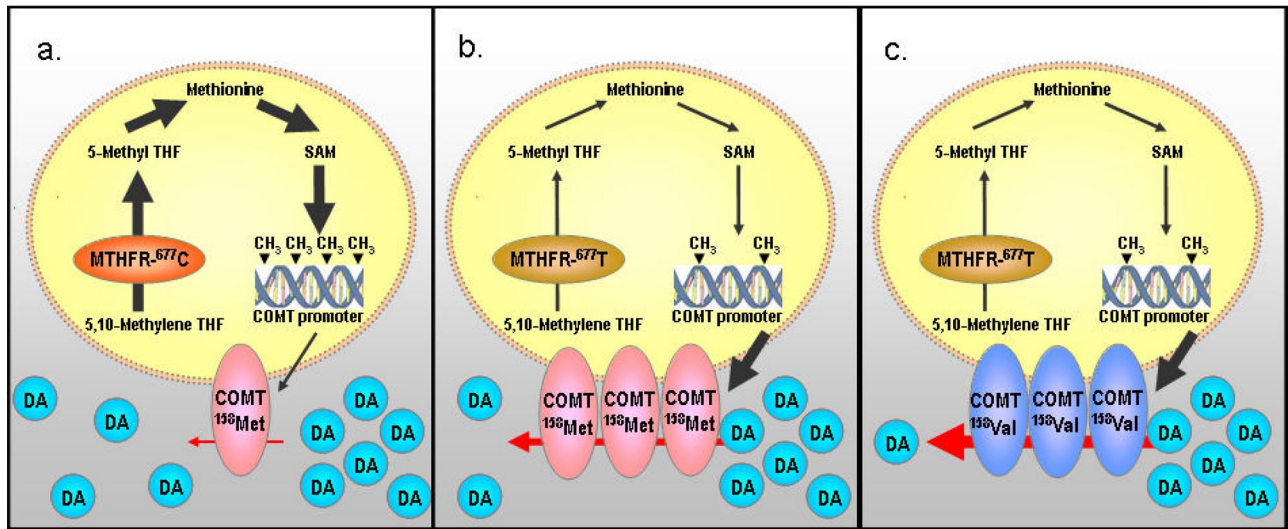


Fig. S4. Proposed interactive effects of MTHFR and COMT genotype on prefrontal dopamine availability. (a) Maximum dopamine availability is predicted among individuals with both the COMT 158Met allele, associated with decreased dopamine turnover, and the MTFHR 677C allele, putatively associated with increased COMT promoter methylation (and thus decreased COMT expression). (b) In the presence of the MTHFR 677T allele, COMT promoter methylation is decreased, COMT expression is increased, and availability of prefrontal dopamine is reduced. (c) With both the MTHFR 677T and COMT 158Val alleles, not only is more COMT expressed, but dopamine availability is further diminished because of the high-activity Val variant [figure modified from Roffman JL, et al. (2007) *Schizophr Res* 92:181–188]. DA, dopamine; THF, tetrahydrofolate; SAM, s-adenosylmethionine.

Table S1. Effect of race on DLPFC recruitment (β_{5D} minus β_{1D}) between 1-digit and 5-digit working memory loads

Race	Right DLPFC recruitment	Left DLPFC recruitment
Caucasian, $n = 124$	0.55 ± 0.09	0.98 ± 0.08
Non-Caucasian, $n = 25$	0.78 ± 0.21	1.15 ± 0.19

Groups did not differ significantly for DLPFC recruitment in either hemisphere. Five participants did not disclose race and were excluded from this analysis. Values indicate mean \pm standard error.

Table S2. Effects of diagnosis and genotype on SIRP accuracy and reaction time (RT) at 1-digit (1D) and 5-digit (5D) working memory loads

Test group	Healthy controls						Schizophrenia patients						All con.	All pat.
	Val/Val		Val/Met		Met/Met		Val/Val		Val/Met		Met/Met			
COMT genotype	T carrier	C/C	T carrier	C/C	T carrier	C/C	T carrier	C/C	T carrier	C/C	T carrier	C/C		
MTHFR genotype	<i>n</i> = 11	<i>n</i> = 11	<i>n</i> = 19	<i>n</i> = 17	<i>n</i> = 10	<i>n</i> = 7	<i>n</i> = 8	<i>n</i> = 9	<i>n</i> = 22	<i>n</i> = 22	<i>n</i> = 8	<i>n</i> = 10	<i>n</i> = 75	<i>n</i> = 79
Accuracy – 1D, %	95.4	98.9	99.1	98.4	99.0	98.1	95.9	95.7	96.7	97.6	95.0	95.9	98.4	96.5
Accuracy – 5D, %	95.8	98.2	98.5	98.1	96.9	97.3	94.4	94.5	93.6	93.2	92.3	94.7	97.7	93.7
	<i>n</i> = 5	<i>n</i> = 6	<i>n</i> = 11	<i>n</i> = 7	<i>n</i> = 9	<i>n</i> = 4	<i>n</i> = 3	<i>n</i> = 6	<i>n</i> = 18	<i>n</i> = 14	<i>n</i> = 7	<i>n</i> = 8	<i>n</i> = 42	<i>n</i> = 56
RT – 1D, msec	616	604	568	562	560	598	596	629	599	623	605	636	579	615
RT – 5D, msec	713	740	706	698	725	758	736	786	789	820	852	830	719	807

RT data is available on a smaller number of subjects due to a data acquisition problem at one site. Repeated measures ANOVA indicated a main effect of working memory load on accuracy, with greater accuracy at 1D than 5D ($F = 27.25, P < 0.001$), and a main effect of diagnosis, with patients making more errors than controls ($F = 9.15, P < 0.001$). There was also a significant load \times diagnosis interaction ($F = 10.10, P = 0.002$), with patients showing a stronger detrimental effect of increased load on accuracy than controls. Similarly, for RT, there was a main effect of working memory load, with greater RT at 5D than 1D ($F = 288, P < 0.001$), and of diagnosis, with patients showing longer RT ($F = 3.63, P = 0.031$). There was again a significant load \times diagnosis interaction ($F = 6.35, P = 0.014$), with patients showing a stronger detrimental effect of increased load on RT than controls. However, genotype did not influence performance, as there were no significant load \times MTHFR, load \times COMT, load \times diagnosis \times MTHFR, load \times diagnosis \times COMT, or load \times diagnosis \times MTHFR \times COMT interactions for either accuracy or RT (all $P > 0.05$).

Table S3. Effects of MTHFR and MTHFR × COMT genotype on DLPFC recruitment ($\beta_{5D} - \beta_{1D}$) in patients and controls

Test group MTHFR genotype	Right DLPFC recruitment		Left DLPFC recruitment	
	C/C	T carrier	C/C	T carrier
All patients, <i>n</i> = 79	0.82 ± 0.16	0.43 ± 0.17	1.42 ± 0.14	0.68 ± 0.15
Val/Val, <i>n</i> = 17	1.01 ± 0.33	<i>-0.23 ± 0.35</i>	1.56 ± 0.30	0.17 ± 0.32
Val/Met, <i>n</i> = 44	1.01 ± 0.21	0.61 ± 0.21	1.45 ± 0.19	0.73 ± 0.19
Met/Met, <i>n</i> = 18	<i>0.23 ± 0.32</i>	<i>0.59 ± 0.35</i>	1.26 ± 0.29	1.03 ± 0.32
All controls, <i>n</i> = 75	0.56 ± 0.17	0.50 ± 0.16	0.97 ± 0.15	0.88 ± 0.14
Val/Val, <i>n</i> = 22	<i>0.72 ± 0.30</i>	<i>0.72 ± 0.30</i>	1.25 ± 0.27	0.97 ± 0.27
Val/Met, <i>n</i> = 36	0.53 ± 0.24	0.05 ± 0.23	0.99 ± 0.22	0.64 ± 0.21
Met/Met, <i>n</i> = 17	<i>0.40 ± 0.38</i>	<i>1.11 ± 0.32</i>	<i>0.48 ± 0.34</i>	<i>1.21 ± 0.29</i>

For each pair of C/C versus T carrier groups, values shown in bold indicate greater recruitment in C/C subjects (C/C > T carriers), and values shown in italic indicate greater recruitment in T carriers (T carriers > C/C). In the left DLPFC, there was a significant main effect of MTHFR genotype (C/C > T carriers, $F = 10.14$, $P = 0.002$) and a significant genotype × diagnosis interaction (MTHFR effects more pronounced in patients, $F = 8.13$, $P = 0.005$). There was also a trend-level significant MTHFR × COMT genotype interaction ($F = 2.31$, $P = 0.10$) and a significant MTHFR × COMT × diagnosis interaction ($F = 3.14$, $P = 0.047$). Trend-level interactions of MTHFR × COMT ($F = 2.95$, $P = 0.056$) and MTHFR × COMT × diagnosis ($F = 2.91$, $P = 0.058$) were also seen in the right DLPFC. Values indicate mean ± standard error.